

This is the accepted manuscript (postprint) of the following article:

R. Keihan, E. Salahinejad, *Inorganic-salt coprecipitation synthesis, fluoride-doping, bioactivity and physiological pH buffering evaluations of bredigite*, *Ceramics International*, 46 (2020) 13292-13296.

<https://doi.org/10.1016/j.ceramint.2020.02.107>

Inorganic-salt coprecipitation synthesis, fluoride-doping, bioactivity and physiological pH buffering evaluations of bredigite

R. Keihan, E. Salahinejad*

Faculty of Materials Science and Engineering, K. N. Toosi University of Technology, Tehran, Iran

Abstract

Bredigite ($\text{Ca}_7\text{MgSi}_4\text{O}_{16}$), with suitable bioactivity, biodegradation, biocompatibility and mechanical properties, is a promising candidate for the repair and regeneration of damaged bone tissues. In this research, for the first time, bredigite was synthesized by a facile and inexpensive coprecipitation method using inorganic salt precursors, followed by calcination at 1200°C . Additionally, 0.5 mol% fluoride was successfully doped into the structure without the formation of any second phases. X-ray diffraction and Fourier-transform infrared spectroscopy confirmed the formation of single-phase orthorhombic bredigite in the samples and the incorporation of fluoride in the doped sample, respectively. Both the undoped and doped samples exhibited apatite-formation ability in terms of the precipitation of hydroxycarbonate apatite when exposed to a simulated physiochemical medium, with an increase in this characteristic as a result of fluoride doping. The addition of fluoride also lowered and buffered the pH value of the medium, where the enhancement of this parameter is due to the fast bioresorption of bredigite affecting disadvantageously biocompatibility.

Keywords: Calcination (A); Silicate (D); Biomedical applications (E)

* Corresponding Author: Email Address: <salahinejad@kntu.ac.ir>

This is the accepted manuscript (postprint) of the following article:

R. Keihan, E. Salahinejad, *Inorganic-salt coprecipitation synthesis, fluoride-doping, bioactivity and physiological pH buffering evaluations of bredigite*, *Ceramics International*, 46 (2020) 13292-13296.

<https://doi.org/10.1016/j.ceramint.2020.02.107>

1. Introduction

Bioactive and biodegradable ceramic powders, granulates, microspheres, scaffolds and blocks are promising candidates for the repair and regeneration of damaged hard tissues. In this regard, the different types of glass, glass-ceramic and crystalline silicates and calcium phosphates (apatites) are noticeable. Among them, bredigite with the chemical composition of $\text{Ca}_7\text{MgSi}_4\text{O}_{16}$, orthorhombic crystalline structure and the density of almost 3.4 g/cm^3 offers considerable bioactivity, biodegradation and more importantly mechanical properties due to its composition and structure [1-3]. Nonetheless, the further development of bredigite as a typical Ca-Mg silicate ceramic in regenerative medicine demands two major considerations from synthesis and biocompatibility viewpoints.

Different chemical and mechanical techniques, including sol-gel [3-5], combustion [6] and ball milling [7-9] have been previously reported to synthesize bredigite. The mechanical activation route leaves a level of contamination in the product, which is deteriorous for medical applications. The wet-chemical synthesis methods reported in the literature are involved with the obligatory use of catalysts, some expensive precursors and time-consuming steps to obtain a single-phase bredigite structure [3-6]. On the other hand, the low concentration of silicon and thereby bridging oxygens provide a higher degradation rate for bredigite in physiological media, compared to other members of Mg-Ca silicates like diopside and akermanite. This results in an excessive enhancement of pH in the media and thereby an inhibiting influence on cell proliferation and metabolism [10], despite a beneficial antibacterial contribution [11-13].

In order to overcome the aforementioned challenges related to production, a straightforward coprecipitation process using inexpensive inorganic salt precursors was introduced to synthesize bredigite in this work. The undesirable increase of pH of the

This is the accepted manuscript (postprint) of the following article:

R. Keihan, E. Salahinejad, *Inorganic-salt coprecipitation synthesis, fluoride-doping, bioactivity and physiological pH buffering evaluations of bredigite*, *Ceramics International*, 46 (2020) 13292-13296.

<https://doi.org/10.1016/j.ceramint.2020.02.107>

physiological media due to the degradation of bredigite was also controlled by fluoride doping, for the first time, while improving the apatite-formation ability of bredigite.

2. Materials and methods

A coprecipitation route, similar to that successfully used for diopside synthesis [14, 15], was employed to prepare pure and fluoride-doped bredigite. Based on the bredigite stoichiometry, an equimolar content of calcium chloride (CaCl_2 , Merck, >98%) and magnesium chloride (MgCl_2 , Merck, >98%) was dissolved in ethanol ($\text{C}_2\text{H}_5\text{OH}$, Merck, >99.9%). For fluoride-doping at 0.5 and 1 mol% into the bredigite structure, 7 and 14 mol% of MgCl_2 were replaced with magnesium fluoride (MgF_2 , Alfa Aesar, >99%). The proper amount of silicon tetrachloride (SiCl_4 , Merck, >99%) was then added to the solution, while keeping the temperature at 0 °C using an ice-water bath. Then, ammonia solution (NH_4OH , Merck, 25%) was dropwise added to the solution to increase pH until 10. The obtained precipitates were several times washed with distilled water, dried at 120 °C and then calcined at 550, 750, 1000 and 1200 °C.

The structure of the undoped and doped powder samples was characterized by X-ray diffraction (XRD, PANalytical X'Pert PRO MPD), Fourier-transform infrared spectroscopy (FTIR, Spectrum 400, Perkin Elmer) and field-emission scanning electron microscopy (FESEM, MIRA3TESCAN-XMU, 15 kV). To study the apatite-formation ability of the samples, the powders were exposed to the simulated body fluid (SBF) at 37 °C. Then, the soaked powders were again investigated by FESEM coupled with energy dispersive X-ray spectroscopy (EDS) and FTIR. In addition, the pH value of the SBF in contact with the synthesized powders was daily measured.

This is the accepted manuscript (postprint) of the following article:

R. Keihan, E. Salahinejad, *Inorganic-salt coprecipitation synthesis, fluoride-doping, bioactivity and physiological pH buffering evaluations of bredigite*, *Ceramics International*, 46 (2020) 13292-13296.

<https://doi.org/10.1016/j.ceramint.2020.02.107>

3. Results and discussion

Fig. 1(a) to (d) shows the XRD pattern of the undoped powders after calcination at the different temperatures. The calcination temperatures of 550 and 750 °C form low-crystallinity structures, as inferred from the low intensity of the XRD peaks. The powder calcined at 1000 °C, however, exhibits a considerable level of crystallinity, albeit with some impurity phases (akermanite- $\text{Ca}_2\text{MgSi}_2\text{O}_7$ - and calcium silicate- Ca_2SiO_4 -) apart from bredigite. Desirably, the calcination temperature of 1200 °C develops a single-phase structure of bredigite with no secondary phases. In this sample, the mean crystallite size of bredigite is estimated to be about 42 nm, based on the Scherrer equation [16], due to the fact that crystals are formed from an amorphous coprecipitation-derived matrix in a bottom-up approach during calcination.

The XRD pattern of the samples doped with the various amounts of fluoride after calcination at 1200 °C is also indicated in Fig. 1(e) and (f). According to the analysis by PANalytical X'Pert software, doping for 0.5 mol% does not change the phase singularity of bredigite, but somewhat increases the intensity and sharpness of the main diffraction peak ($2\theta=33.5^\circ$) due to the increase in crystallinity and crystallite size (almost 55 nm). This is attributed to a decrease of melting point which equals 1372 °C [1] as a result of the partial substitution of fluoride for oxygen [17-20] and thereby an increase in the homologous temperature of calcination at 1200 °C. However, 1 mol% fluoride incorporation dominates the akermanite and diopside ($\text{MgCaSi}_2\text{O}_6$) phases rather than bredigite. Thus, only 0.5 mol% fluoride-doped sample is hereafter considered to study the effect of fluoride on the structural and biological characteristics of bredigite.

Fig. 2 demonstrates the FTIR spectra of the pure and fluoride-doped samples calcined at 1200 °C. For the undoped sample, the detection of O-Ca-O, O-Mg-O and Si-O vibrations,

This is the accepted manuscript (postprint) of the following article:

R. Keihan, E. Salahinejad, *Inorganic-salt coprecipitation synthesis, fluoride-doping, bioactivity and physiological pH buffering evaluations of bredigite*, *Ceramics International*, 46 (2020) 13292-13296.

<https://doi.org/10.1016/j.ceramint.2020.02.107>

compatible with Refs. [3, 10, 21], is indicative of Ca-Mg silicate (bredigite). Fluoride doping reflects three characteristic differences in the FTIR spectrum of bredigite. First, a new broad peak is created in the FTIR spectrum of the doped sample, which is assigned to Si-F. Second, the peak intensity of the functional groups of bredigite, i.e. O-Ca-O, O-Mg-O and Si-O, exhibits a decrease after fluoride doping. Third, the doping process shifts the functional group peaks to higher wavenumbers. The evolution of the peak intensities and positions after doping is due to the partial replacement of oxygen with fluoride, converting a number of O-Ca-O, O-Mg-O and Si-O to O-Ca-F, O-Mg-F and Si-F, respectively. These variations with fluoride doping are in agreement with other fluoride-doped ceramics reports [22-25].

The FESEM micrograph of the powders calcined at 750 °C is depicted in Fig. 3. As can be seen, the undoped and doped powder samples are composed of well-dispersed nanoparticles of about 60 and 140 nm in mean size, respectively. After calcination at 1200 °C to obtain the homogeneous bredigite structures characterized by the XRD analysis, the powder particles are coarsened to 1-2 µm, agglomerated and even sintered (Fig. 4). The development of sintering necks is more evidently observed for the doped sample, since the fluoride incorporation is expected to decrease the melting point of silicates [17-20] and thereby to increase sinterability at a given calcination/sintering temperature. These variations are compatible with fluoride-doped diopside as another typical member of Mg-Ca silicates [18, 26].

Fig. 5 represents the FESEM micrograph and EDS spectrum of the powders after immersion in the SBF. As a criterion of bioactivity, apatite-like precipitates can be observed on the powder surfaces, where the level of the precipitates on the doped sample is more than the pure sample. Also, the peak intensity of phosphorous in the EDS profiles for the doped sample is higher than that for the undoped sample. That is, both the FESEM and EDS

This is the accepted manuscript (postprint) of the following article:

R. Keihan, E. Salahinejad, *Inorganic-salt coprecipitation synthesis, fluoride-doping, bioactivity and physiological pH buffering evaluations of bredigite*, *Ceramics International*, 46 (2020) 13292-13296.

<https://doi.org/10.1016/j.ceramint.2020.02.107>

analyses confirm that the apatite-formation ability of bredigite is enhanced by fluoride doping. The well-established ion-exchange mechanism of Ca-Mg silicates [27-29] explains the bioactivity of bredigite.

The FTIR spectra of the samples after soaking in the SBF are displayed in Fig. 6. The detection of PO_4^{3-} and CO_3^{2-} vibrations, in agreement with Refs. [3, 30, 31], suggests that the precipitations deposited on the powder samples are hydroxycarbonate apatite. The higher number of the PO_4^{3-} vibrations for the doped powder confirms the higher apatite-formation ability of this sample than the undoped sample, as concluded from the FESEM-EDS analyses. It is also detected that fluoride doping slightly shifts the peaks of the functional groups to higher wavenumbers for about 3-5 cm^{-1} . This infers the partial incorporation of fluoride into the precipitated apatite phase, which enhances the chemical stability of apatite against dissolution towards the medium and explains the bioactivity improvement with fluoride doping. Albeit at high levels of fluoride incorporation, the formation of fluorite (CaF_2) consumes calcium and accordingly limits the deposition of apatite [30, 32, 33].

Fig. 7 presents the pH value of the SBF after exposure to the synthesized powder samples. For both the samples in comparison to the reference (the SBF in contact with no samples), pH exhibits a sharp increase to 1st day, followed by a slow enhancement to 4th day of soaking. From 4th day to 14th day, however, pH presents the relatively constant values of 9.5 and 8.7 for the undoped and doped samples, respectively. The first increase in pH is attributed to the fast release of Ca^{2+} and Mg^{2+} from the bioceramics towards the SBF and in return the adsorption of H^+ and H_3O^+ of the SBF on the sample surface to balance the electrical charge. This ion exchange reaction decreases the concentration of H^+ in the SBF and hence increases pH. The constant value of pH after 4th day is because of a balance between the ceramic dissolution and apatite deposition, where the former increases pH and

This is the accepted manuscript (postprint) of the following article:

R. Keihan, E. Salahinejad, *Inorganic-salt coprecipitation synthesis, fluoride-doping, bioactivity and physiological pH buffering evaluations of bredigite*, *Ceramics International*, 46 (2020) 13292-13296.

<https://doi.org/10.1016/j.ceramint.2020.02.107>

the latter decreases it due to the adsorption of hydroxyl group (OH⁻) of the SBF to form hydroxycarbonate apatite. It is also noticeable that over the entire range of the pH measurements, pH for the doped sample is lower than that for the pure bredigite powder. This is attributed to the exchange of F⁻ of the bioceramic with OH⁻ of the SBF, thereby decreasing the concentration of hydroxyl in the SBF. This pH buffering effect as a result of doping is remarkable because one of the important challenges to further develop bredigite for biomedical applications is the excessive enhancement of physiological pH [10].

4. Conclusions

In this work, bredigite was successfully synthesized by a novel coprecipitation technique using inorganic precursors, followed by calcination. With the target of obtaining the phase singularity, 0.5 mol% fluoride was also doped successfully into bredigite, whereas 1 mol% incorporation did not develop a single-phase structure. Fluoride doping at 0.5 mol% level enhanced the apatite-formation ability of bredigite, in terms of the precipitation of hydroxycarbonate apatite when exposed to the SBF. The pH value of the SBF in contact with the synthesized powders was increased to almost 9, where fluoride doping somewhat buffered this parameter. It is finally concluded that fluoride doping of bredigite can be used to modify the biological performance of this bioceramic.

References

- [1] M. Diba, O.-M. Goudouri, F. Tapia, A.R. Boccaccini, Magnesium-containing bioactive polycrystalline silicate-based ceramics and glass-ceramics for biomedical applications, *Current opinion in solid state and materials science*, 18 (2014) 147-167.
- [2] H. Ghomi, R. Emadi, Fabrication of bioactive porous bredigite (Ca₇MgSi₄O₁₆) scaffold via space holder method, *International Journal of Materials Research*, 109 (2018) 257-264.

This is the accepted manuscript (postprint) of the following article:

R. Keihan, E. Salahinejad, *Inorganic-salt coprecipitation synthesis, fluoride-doping, bioactivity and physiological pH buffering evaluations of bredigite*, *Ceramics International*, 46 (2020) 13292-13296.
<https://doi.org/10.1016/j.ceramint.2020.02.107>

- [3] M. Rahmati, M. Fathi, M. Ahmadian, Preparation and structural characterization of bioactive bredigite (Ca₇MgSi₄O₁₆) nanopowder, *Journal of Alloys and Compounds*, 732 (2018) 9-15.
- [4] C. Wu, J. Chang, J. Wang, S. Ni, W. Zhai, Preparation and characteristics of a calcium magnesium silicate (bredigite) bioactive ceramic, *Biomaterials*, 26 (2005) 2925-2931.
- [5] C. Wu, J. Chang, Synthesis and in vitro bioactivity of bredigite powders, *Journal of biomaterials applications*, 21 (2007) 251-263.
- [6] X.-H. Huang, J. Chang, Preparation of nanocrystalline bredigite powders with apatite-forming ability by a simple combustion method, *Materials Research Bulletin*, 43 (2008) 1615-1620.
- [7] F. Tavangarian, R. Emadi, Mechanism of nanostructure bredigite formation by mechanical activation with thermal treatment, *Materials Letters*, 65 (2011) 2354-2356.
- [8] A. Khandan, N. Ozada, Bredigite-Magnetite (Ca₇MgSi₄O₁₆-Fe₃O₄) nanoparticles: A study on their magnetic properties, *Journal of Alloys and Compounds*, 726 (2017) 729-736.
- [9] S. Sahmani, A. Khandan, S. Saber-Samandari, M. Aghdam, Nonlinear bending and instability analysis of bioceramics composed with magnetite nanoparticles: Fabrication, characterization, and simulation, *Ceramics International*, 44 (2018) 9540-9549.
- [10] C. Wu, J. Chang, Degradation, bioactivity, and cytocompatibility of diopside, akermanite, and bredigite ceramics, *Journal of Biomedical Materials Research Part B: Applied Biomaterials: An Official Journal of The Society for Biomaterials, The Japanese Society for Biomaterials, and The Australian Society for Biomaterials and the Korean Society for Biomaterials*, 83 (2007) 153-160.
- [11] D. He, C. Zhuang, C. Chen, S. Xu, X. Yang, C. Yao, J. Ye, C. Gao, Z. Gou, Rational Design and Fabrication of Porous Calcium–Magnesium Silicate Constructs That Enhance Angiogenesis and Improve Orbital Implantation, *ACS Biomaterials Science & Engineering*, 2 (2016) 1519-1527.
- [12] Y. Shen, Z. Wang, J. Wang, Y. Zhou, H. Chen, C. Wu, M. Haapasalo, Bifunctional bioceramics stimulating osteogenic differentiation of a gingival fibroblast and inhibiting plaque biofilm formation, *Biomaterials science*, 4 (2016) 639-651.
- [13] S. Hu, C. Ning, Y. Zhou, L. Chen, K. Lin, J. Chang, Antibacterial activity of silicate bioceramics, *Journal of Wuhan University of Technology-Mater. Sci. Ed.*, 26 (2011) 226-230.
- [14] E. Salahinejad, R. Vahedifard, Deposition of nanodiopside coatings on metallic biomaterials to stimulate apatite-forming ability, *Materials & Design*, 123 (2017) 120-127.
- [15] N. Namvar, E. Salahinejad, A. Saberi, M.J. Baghjehaz, L. Tayebi, D. Vashaei, Toward reducing the formation temperature of diopside via wet-chemical synthesis routes using chloride precursors, *Ceramics International*, 43 (2017) 13781-13785.
- [16] U. Holzwarth, N. Gibson, The Scherrer equation versus the 'Debye-Scherrer equation', *Nature nanotechnology*, 6 (2011) 534.
- [17] D.S. Brauer, N. Karpukhina, M.D. O'Donnell, R.V. Law, R.G. Hill, Fluoride-containing bioactive glasses: effect of glass design and structure on degradation, pH and apatite formation in simulated body fluid, *Acta Biomaterialia*, 6 (2010) 3275-3282.
- [18] M.J. Baghjehaz, E. Salahinejad, Enhanced sinterability and in vitro bioactivity of diopside through fluoride doping, *Ceramics International*, 43 (2017) 4680-4686.
- [19] D.S. Brauer, N. Karpukhina, R.V. Law, R.G. Hill, Structure of fluoride-containing bioactive glasses, *Journal of Materials Chemistry*, 19 (2009) 5629-5636.
- [20] A. Rafferty, A. Clifford, R. Hill, D. Wood, B. Samuneva, M. Dimitrova-Lukacs, Influence of fluorine content in apatite–mullite glass-ceramics, *Journal of the American Ceramic Society*, 83 (2000) 2833-2838.
- [21] M. Kouhi, M. Fathi, V.J. Reddy, S. Ramakrishna, Bredigite Reinforced Electrospun Nanofibers for Bone Tissue Engineering, *Materials Today: Proceedings*, 7 (2019) 449-454.
- [22] M. Reiche, M. Wiegand, U. Gösele, Infrared spectroscopic analysis of plasma-treated Si (100)-surfaces, *Microchimica Acta*, 133 (2000) 35-43.

This is the accepted manuscript (postprint) of the following article:

R. Keihan, E. Salahinejad, *Inorganic-salt coprecipitation synthesis, fluoride-doping, bioactivity and physiological pH buffering evaluations of bredigite*, *Ceramics International*, 46 (2020) 13292-13296.
<https://doi.org/10.1016/j.ceramint.2020.02.107>

- [23] P.J. Launer, Infrared analysis of organosilicon compounds: spectra-structure correlations, *Silicone compounds register and review*, 100 (1987).
- [24] W.D. Brown, *Dielectric Material Integration for Microelectronics*, The Electrochemical Society, 1998.
- [25] W. Peng-Fei, D. Shi-Jin, Z. Wei, Z. Jian-Yun, W. Ji-Tao, L.W. Wei, FTIR Characterization of fluorine doped silicon dioxide thin films deposited by plasma enhanced chemical vapor deposition, *Chinese Physics Letters*, 17 (2000) 912.
- [26] M. Shahrouzifar, E. Salahinejad, E. Sharifi, Co-incorporation of strontium and fluorine into diopside scaffolds: Bioactivity, biodegradation and cytocompatibility evaluations, *Materials Science and Engineering: C*, 103 (2019) 109752.
- [27] R. Vahedifard, E. Salahinejad, Microscopic and spectroscopic evidences for multiple ion-exchange reactions controlling biomineralization of CaO. MgO. 2SiO₂ nanoceramics, *Ceramics International*, 43 (2017) 8502-8508.
- [28] H. Rahmani, E. Salahinejad, Incorporation of monovalent cations into diopside to improve biomineralization and cytocompatibility, *Ceramics International*, 44 (2018) 19200-19206.
- [29] M. Shahrouzifar, E. Salahinejad, Strontium doping into diopside tissue engineering scaffolds, *Ceramics International*, 45 (2019) 10176-10181.
- [30] E. Salahinejad, M.J. Baghjeghaz, Structure, biomineralization and biodegradation of Ca-Mg oxyfluorosilicates synthesized by inorganic salt coprecipitation, *Ceramics International*, 43 (2017) 10299-10306.
- [31] M. Manoj, D. Mangalaraj, N. Ponpandian, C. Viswanathan, Core-shell hydroxyapatite/Mg nanostructures: surfactant free facile synthesis, characterization and their in vitro cell viability studies against leukaemia cancer cells (K562), *RSC Advances*, 5 (2015) 48705-48711.
- [32] P. Taddei, E. Modena, A. Tinti, F. Siboni, C. Prati, M.G. Gandolfi, Effect of the fluoride content on the bioactivity of calcium silicate-based endodontic cements, *Ceramics International*, 40 (2014) 4095-4107.
- [33] N. Esmati, T. Khodaei, E. Salahinejad, E. Sharifi, Fluoride doping into SiO₂-MgO-CaO bioactive glass nanoparticles: bioactivity, biodegradation and biocompatibility assessments, *Ceramics International*, 44 (2018) 17506-17513.

This is the accepted manuscript (postprint) of the following article:

R. Keihan, E. Salahinejad, *Inorganic-salt coprecipitation synthesis, fluoride-doping, bioactivity and physiological pH buffering evaluations of bredigite*, *Ceramics International*, 46 (2020) 13292-13296.

<https://doi.org/10.1016/j.ceramint.2020.02.107>

Figures:

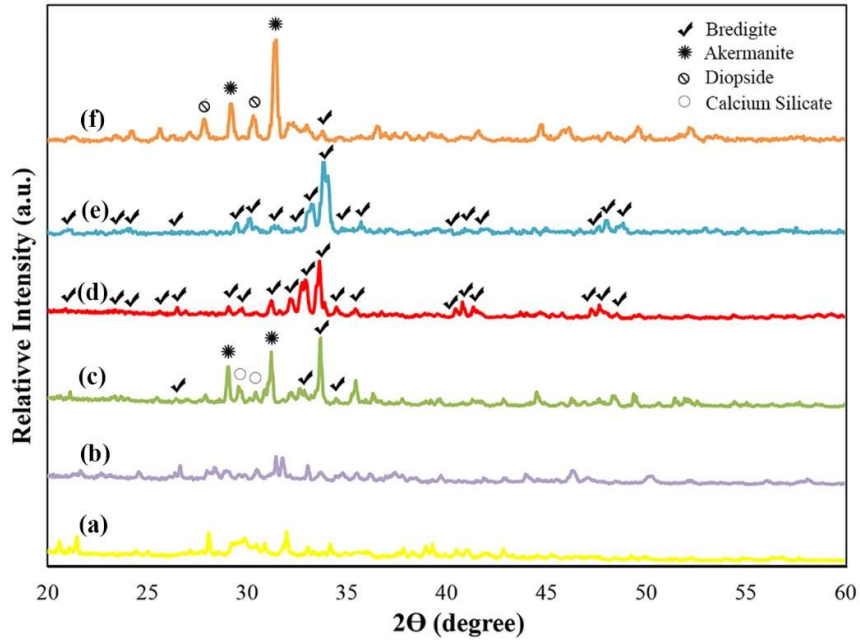


Fig. 1. XRD patterns of the undoped powders after calcination at 550 (a), 750 (b), 1000 (c) and 1200 (d) °C, and of the powders doped with 0.5 (e) and 1 (f) mol% fluoride after calcination at 1200 °C.

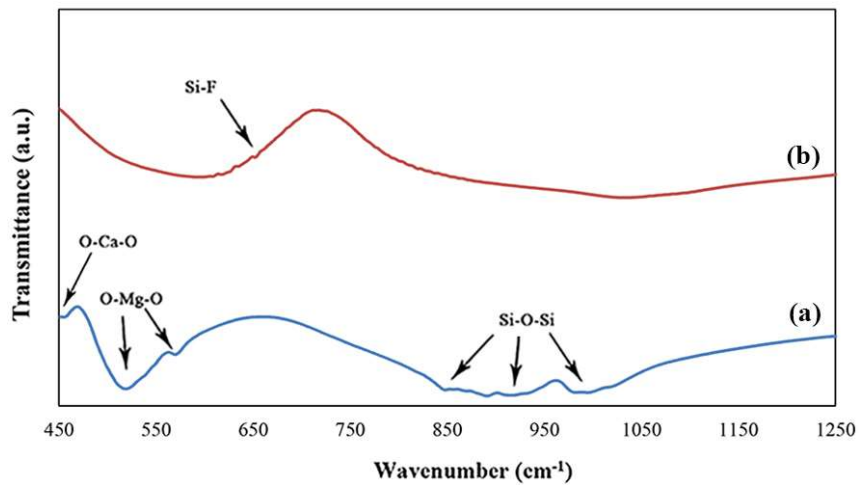


Fig. 2. FTIR spectra of the pure (a) and fluoride-doped (b) samples calcined at 1200 °C.

This is the accepted manuscript (postprint) of the following article:

R. Keihan, E. Salahinejad, *Inorganic-salt coprecipitation synthesis, fluoride-doping, bioactivity and physiological pH buffering evaluations of bredigite*, *Ceramics International*, 46 (2020) 13292-13296.

<https://doi.org/10.1016/j.ceramint.2020.02.107>

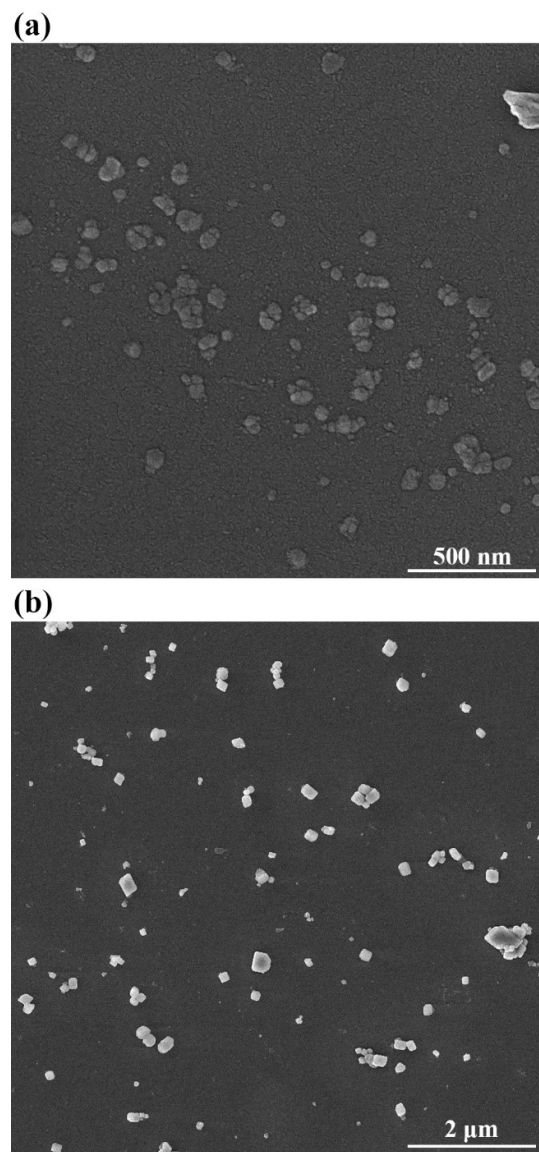


Fig. 3. FESEM micrographs of the pure (a) and fluoride-doped (b) samples calcined at 750 °C.

This is the accepted manuscript (postprint) of the following article:

R. Keihan, E. Salahinejad, *Inorganic-salt coprecipitation synthesis, fluoride-doping, bioactivity and physiological pH buffering evaluations of bredigite*, *Ceramics International*, 46 (2020) 13292-13296.

<https://doi.org/10.1016/j.ceramint.2020.02.107>

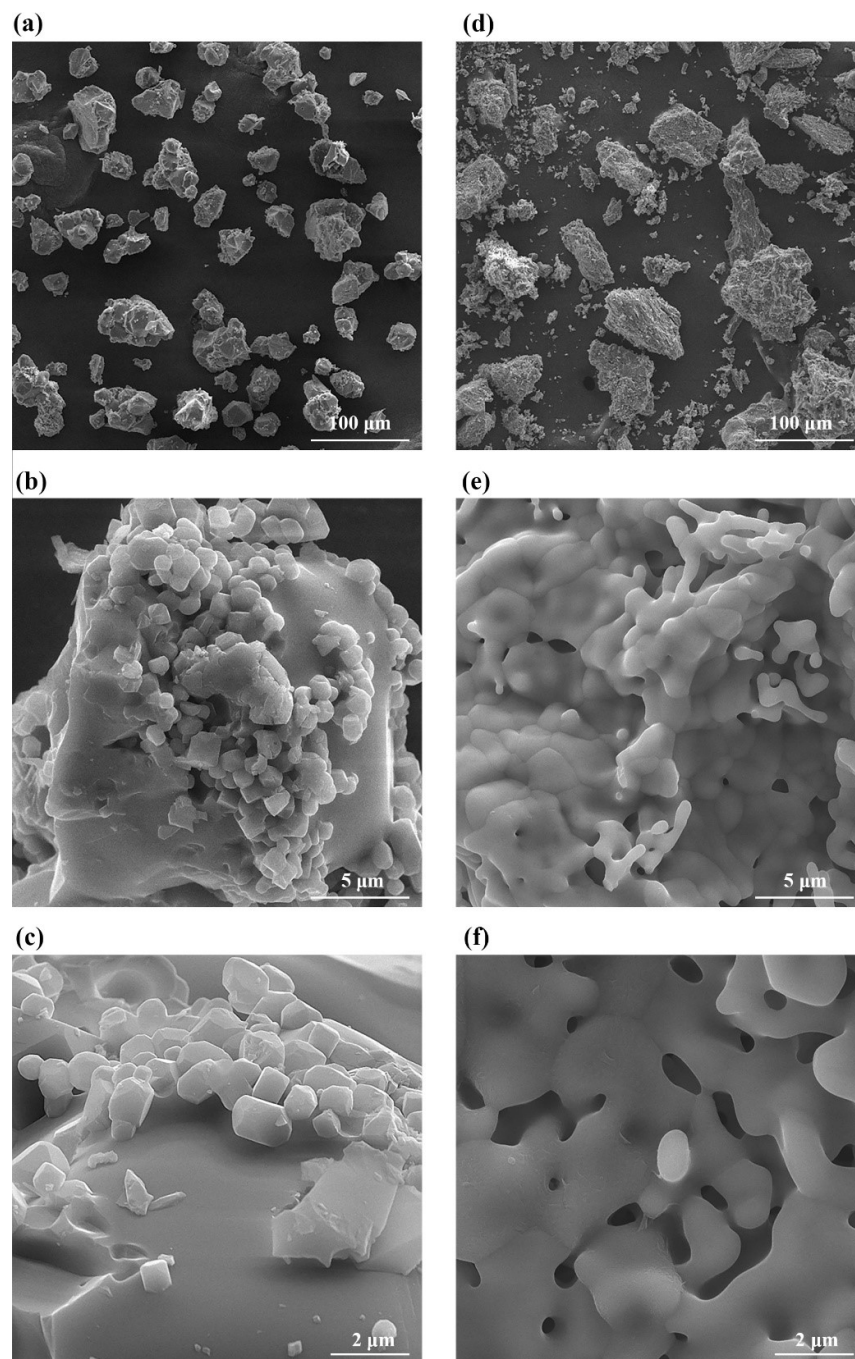


Fig. 4. FESEM micrographs of the pure (a, b, c) and fluoride-doped (d, e, f) samples calcined at 1200 °C.

This is the accepted manuscript (postprint) of the following article:

R. Keihan, E. Salahinejad, *Inorganic-salt coprecipitation synthesis, fluoride-doping, bioactivity and physiological pH buffering evaluations of bredigite*, *Ceramics International*, 46 (2020) 13292-13296.

<https://doi.org/10.1016/j.ceramint.2020.02.107>

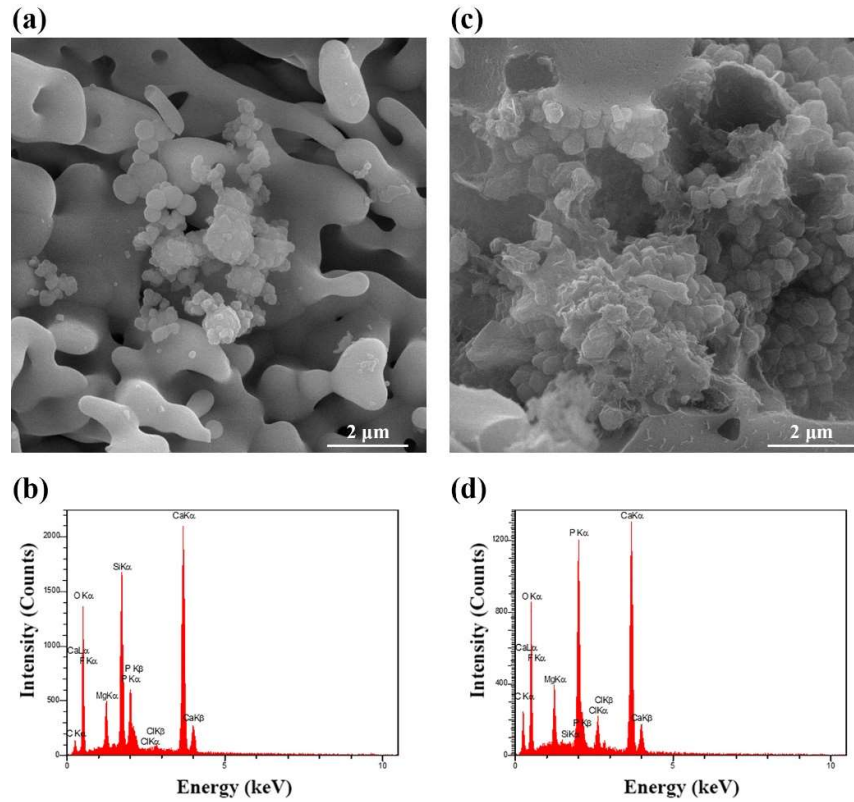


Fig. 5. FESEM micrographs and EDS spectra of the pure (a, b) and fluoride-doped (c, d) samples calcined at 1200 °C after soaking in the SBF.

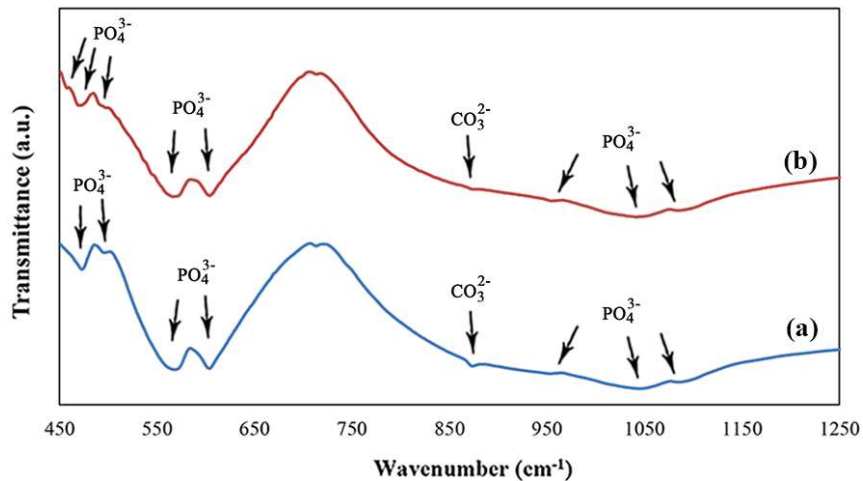


Fig. 6. FTIR spectra of the pure (a) and fluoride-doped (b) samples calcined at 1200 °C after immersion in the SBF.

This is the accepted manuscript (postprint) of the following article:

R. Keihan, E. Salahinejad, *Inorganic-salt coprecipitation synthesis, fluoride-doping, bioactivity and physiological pH buffering evaluations of bredigite*, *Ceramics International*, 46 (2020) 13292-13296.

<https://doi.org/10.1016/j.ceramint.2020.02.107>

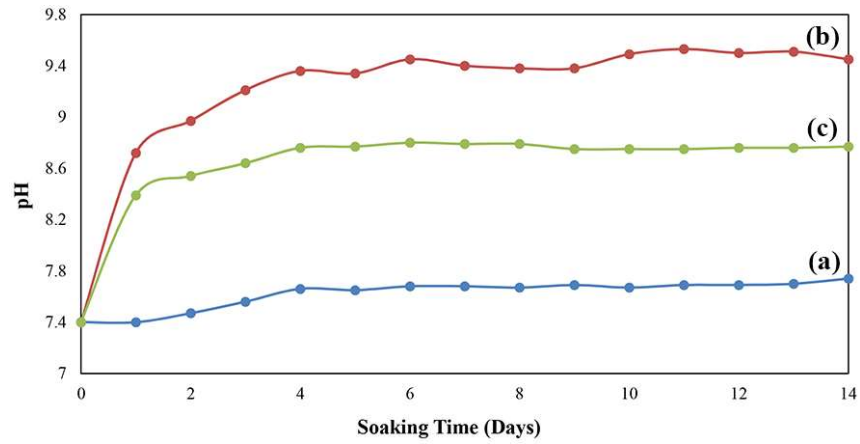


Fig. 7. pH variations of the SBF in contact with no (a), undoped (b) and doped (c) samples calcined at 1200 °C.